KPAC: A Kernel-Based Parametric Active Contour Method for Fast Image Segmentation

Akshaya Mishra and Alexander Wong

***Abstract*—Object boundary detection has been a topic of keen interest to the signal processing and pattern recognition community. A popular approach for object boundary detection is parametric active contours. Existing parametric active contour approaches often suffer from slower convergence rates, difficulty dealing with complex high curvature boundaries, and are prone to being trapped in local optima in the presence of noise and background clutter. To address these problems, this paper proposes a novel kernel-based active contour (KPAC) approach, which replaces the conventional internal energy term used in existing approaches by incorporating an adaptive kernel derived for the underlying image characteristics. Experimental results demonstrate that the KPAC approach achieves state-of-the-art performance when compared to two other state-of-the-art parametric active contour approaches.**

***Index Terms*—Boundary extraction, kernel, parametric active contour.**

I. Introduction

ROBUST identification of object boundaries in the presence of noise and background clutter has many important applications in biomedical engineering [1], [2], visual tracking [3], content based image and video retrieval [4], video segmentation [5], and image composition [6]. A popular approach to object boundary detection are those based on active contours [7]–[14]. Existing parametric active contour approaches iteratively evolve a deformable model to minimize the sum of internal and external energies of the model to obtain an optimal curve representing the object boundary. The internal energy enforces a penalty on the slope and curvature of the object boundary, while the external energy pulls the deformable model towards the object boundary. Many variations of the traditional active contour approach [7] proposed have focused on increasing the capture range [15]–[19] of the traditional active contour approach. Further, PCA based training [20] has been attempted to avoid initialization and capture range problem.

There are three major challenges currently faced by parametric active contour approaches for object boundary detection. The first major challenge deals with slow convergence rate, particularly when faced with complex imagery. The second major challenge deals with the presence of image noise contamination and background clutter, which can lead to poor boundary detection accuracy due to convergence to local optima. Third, existing approaches have difficulty dealing with complex high curvature boundaries. To address these issues, this paper proposes a novel kernel-based parametric active contour (KPAC) method, that shares the same underlying theory of traditional deformable models. However, instead of employing penalties on slope and curvature as an internal energy, which are highly sensitive to noise and handles high curvature boundaries poorly, KPAC introduces an adaptive non-stationary kernel, derived from the underlying image characteristics, as the internal energy of the deformable model. This approach allows the faster and more accurate convergence by adapting to the underlying image characteristics, particularly under situations characterized by noise and complex high curvature boundaries.

Manuscript received September 09, 2009; revised November 02, 2009. First published November 13, 2009; current version published February 03, 2010. This work was supported in part by the Natural Sciences and Engineering Research Council (NSERC) of Canada and Vision and Image Processing Lab, Systems Design Engineering, University of Waterloo. The associate editor coordinating the review of this manuscript and approving it for publication was Prof. Dimitrios Androutsas.

The authors are with the University of Waterloo, Waterloo, ON Canada N2L 3G1 (e-mail: akmishrau@waterloo.ca ,a28wong@uwaterloo.ca.

Digital Object Identifier 10.1109/LSP.2009.2036654

II. Parametric Active Contour Theory

The seminal work on parametric active contour [7] defined the active contour as an energy minimizing deformable model $v(s) = (x(s), y(s))$, $s \in [0, 1]$, with normalized arclength s. The goal is to evolve the deformable model to minimize the energy functional

$$E = \int_0^1 \left(\underbrace{\alpha(s)v_s^2(s)}_{Elastic} + \underbrace{\beta(s)v_{ss}^2(s)}_{Membrane} - \underbrace{\gamma(s)E_{ext}(v(s))}_{External} \right) ds \tag{1}$$

where $v_s(s)$ and $v_{ss}(s)$ are the first and second derivatives of $v(s)$ with respect to arclength s, and the parameters $\alpha(s)$, $\beta(s)$ and $\gamma(s)$ are the penalties on slope, curvature and the external force, respectively.

The internal energy, representing the prior, is a weighted sum of elastic and membrane energies, whereas the external energy is computed from the image I in a manner dependant upon the application. Typically, as the object boundaries coincide with image edges, the external energy is made a function of the image gradient (g) such that the contour could converge to the boundaries,

$$E_{ext} = g^2(I) = (\delta G_\sigma * I)^2 \tag{2}$$

where $*$ is the convolution operator and δG_σ is the first-order Gaussian derivative.

Using the Euler-Lagrange equation, the minimization of (1) in vector and matrix format can be expressed as

$$A\mathbf{x} + f_{\mathbf{x}}(\mathbf{x}, \mathbf{y}) = 0, \quad A\mathbf{y} + f_{\mathbf{y}}(\mathbf{x}, \mathbf{y}) = 0 \tag{3}$$

where A is a pentadiagonal banded matrix, and f_x and f_y are partial first derivatives of E_{ext} w.r.t. x and y respectively. The iterative solution to (3) using gradient descent optimization can thus be expressed as

$$\mathbf{x}_t = (A+\gamma I)^{-1}\left(\mathbf{x}_{t-1} - f_{\mathbf{x}}(x_{t-1}, y_{t-1})\right) \tag{4}$$

and

$$\mathbf{y}_t = (A+\gamma I)^{-1}\left(\mathbf{y}_{t-1} - f_{\mathbf{y}}(x_{t-1}, y_{t-1})\right). \tag{5}$$

There are two major issues associated with this formulation: 1) slower convergence rate, 2) inability to converge towards high curvature boundaries, and 3) sensitive to local minima under noise and clutter. While methods have been proposed to deal mainly with convergence speed [15], [16], it is important to deal with all three issues concurrently to achieve accurate object boundary detection under various situations. Therefore, to address these issues, KPAC dynamically derives a non-stationary kernel from the underlying image characteristics to account for noise, clutter, and complex high curvature boundaries, as well as better attract the initial contour that is far from the desired solution to improve convergence speed.

III. Kernel-Based Parametric Active Contour (KPAC)

The proposed KPAC approach can be described as follows. Let $\mathbf{v} \in [\mathbf{x}, \mathbf{y}]$ be a deformable model. At the equilibrium [7], when $\mathbf{v}$ lies at the boundary of the object,

$$B\mathbf{v} + f(\mathbf{v}) = 0 \tag{6}$$

where the matrix B defines some internal constraints that defines the properties of the object boundaries, while $f = [f_x, f_y]$ defines some external constraints that ties the boundary to the object boundaries. Therefore, in object boundary detection, the goal is to evolve $\mathbf{v}$ such that (6) is satisfied. Rather than defining an internal constraints matrix B in a stationary, static manner like previous approaches, which is prone to being trapped in local optima under noise, clutter, and complex high curvature boundaries, we instead reformulate the evolution of $\mathbf{v}$ to introduce an adaptive non-stationary kernel K_t to enforce different constraints depending on the underlying image characteristics:

$$\mathbf{v}_t = K_t\left(\mathbf{v}_{t-1} - f\left(\mathbf{v}_{t-1}\right)\right). \tag{7}$$

The individual components of $\mathbf{v}_t = [\mathbf{x}_t, \mathbf{y}_t]$ are define by:

$$\mathbf{x}_t = K_t\left(\mathbf{x}_{t-1} - f_x\left(\mathbf{x}_{t-1}\right)\right). \tag{8}$$

and

$$\mathbf{y}_t = K_t\left(\mathbf{y}_{t-1} - f_y\left(\mathbf{y}_{t-1}\right)\right) \tag{9}$$

where $f_x = \partial g/dy$ and $f_y = \partial g/dy$. Present active contour evolution literature uses a stationary kernel equivalent to

$$K_t = (A+\gamma I)^{-1} \tag{10}$$

that is derived from local neighborhood of each snake coordinates. However, we want a kernel that account for both global feature image features and local spatial features. Therefore, essentially, we need an adaptive kernel K_t that dynamically adjusts the constraints being asserted based on the local neighborhood image characteristics, when the image gradient used by the external energy is insufficient to define the object boundaries. To account for the aforementioned issues associated with noise, clutter, complex high curvature boundaries, and convergence speed, we introduce an adaptive kernel K for a particular pixel $v_i \in \mathbf{v_t}$ that is a product of three different penalties based on local image characteristics of its q neighbors: 1) penalty on gradient deviation (ψ), 2) penalty on spatial deviation (ϕ), and 3) penalty on intensity deviation (φ):

$$K_t(i,j) = \frac{\psi_{t-1}(i,j)\,\phi(i,j)\,\varphi_{t-1}(i,j)}{\sum_{j=1}^{q}\psi_{t-1}(i,j)\,\phi(i,j)\,\varphi_{t-1}(i,j)}, \quad j = \{1,2,3\cdots q\} \tag{11}$$

$$\psi_{t-1}(i,j) = \exp\left(-\frac{\left(g_{t-1}(v(i)) - g_{t-1}(v(j))\right)}{\sigma_{g_{t-1}(\mathbf{v_t})}}\right) \tag{12}$$

and

$$\phi(i,j) = \exp\left(-\frac{|v(i) - (v(j))|_2}{\sigma_{\mathbf{v_{t-1}}}}\right) \tag{13}$$

$$\varphi_{t-1}(i,j) = \exp\left(-\frac{\left(I_{t-1}(v(i)) - I_{t-1}(v(j))\right)}{\sigma_{I_{t-1}(\mathbf{v_{t-1}})}}\right). \tag{14}$$

where $\sigma_{g_{t-1}(\mathbf{v_{t-1}})}$, $\sigma_{\mathbf{v_{t-1}}}$, and $\sigma_{I_{t-1}(\mathbf{v_{t-1}})}$ are regularization constants for the individual penalties. The effect of these three penalty terms in handing background clutter, high curvature and noise are presented in Section IV.

IV. Experimental Results and Discussions

The goal of this section is to investigate the effectiveness of KPAC at accurately identifying object boundaries. To achieve this goal, object boundary detection was performed on a set of four test images without any synthetic noise ($\sigma = 0$), and with additive Gaussian noise of zero mean ($\mu = 0$) and 40 standard deviation ($\sigma = 40$). This set of test images [21] is designed to test the capability of KPAC in handling real images with complex boundary characteristics and background clutter, while the Gaussian noise test cases are designed to test its capabilities at handling situations characterized by high noise levels. For comparison purposes, two popular parametric active contour techniques (gradient vector flow (GVFS) [15] and vector field convolution (VFC) [16]) were also evaluated. The mean square error (MSE) of the detected boundaries from the provided ground truth [21] and execution time is measured for each test case for quantitative comparisons between methods. The tested methods under evaluation were implemented in MATLAB and tested on an Intel Pentium 4 2.4 GHz machine with 1 GB of RAM.

The MSE and execution time for the tested methods are shown in Table I. The proposed KPAC method achieves noticeably lower MSE in all of the test cases and all noise levels when compared to GVFS and VFC, thus demonstrating the ability of KPAC in handling noise, background clutter, and complex boundary characteristics in real images. Furthermore, KPAC has noticeably lower execution time when compared to GVFS

TABLE I
MEAN SQUARE ERROR (MSE) IN PIXELS AND EXECUTION TIME (ET) IN SECONDS OF KPAC COMPARED TO TWO OTHER METHODS FOR FOUR DIFFERENT IMAGES AT TWO NOISE LEVELS. BOLD TEXT INDICATES BEST PERFORMANCE ACROSS ALL METHODS FOR A PARTICULAR IMAGE AT A PARTICULAR NOISE LEVEL.

Mean Square Error [pixels]						
	Without noise			With noise $\sigma = 40, \mu = 0$		
	KPAC	GVFS	VFC	KPAC	GVFS	VFC
FISH	**1.8**	2.1	2.4	**2.7**	6.9	4.1
DUCK	**2.69**	6.98	6.23	**3.28**	8.12	9.62
BOAT	**2.54**	3.22	5.22	**3.60**	10.23	8.61
LEAF	**5.19**	5.42	5.55	**5.94**	11.19	8.15

Execution time (ET) [seconds]					
Without noise			With noise $\sigma = 40, \mu = 0$		
KPAC	GVFS	VFC	KPAC	GVFS	VFC
27	121	61	**33**	151	76
34	134	73	**41**	159	86
38	143	79	**52**	183	97
41	153	92	**59**	203	109

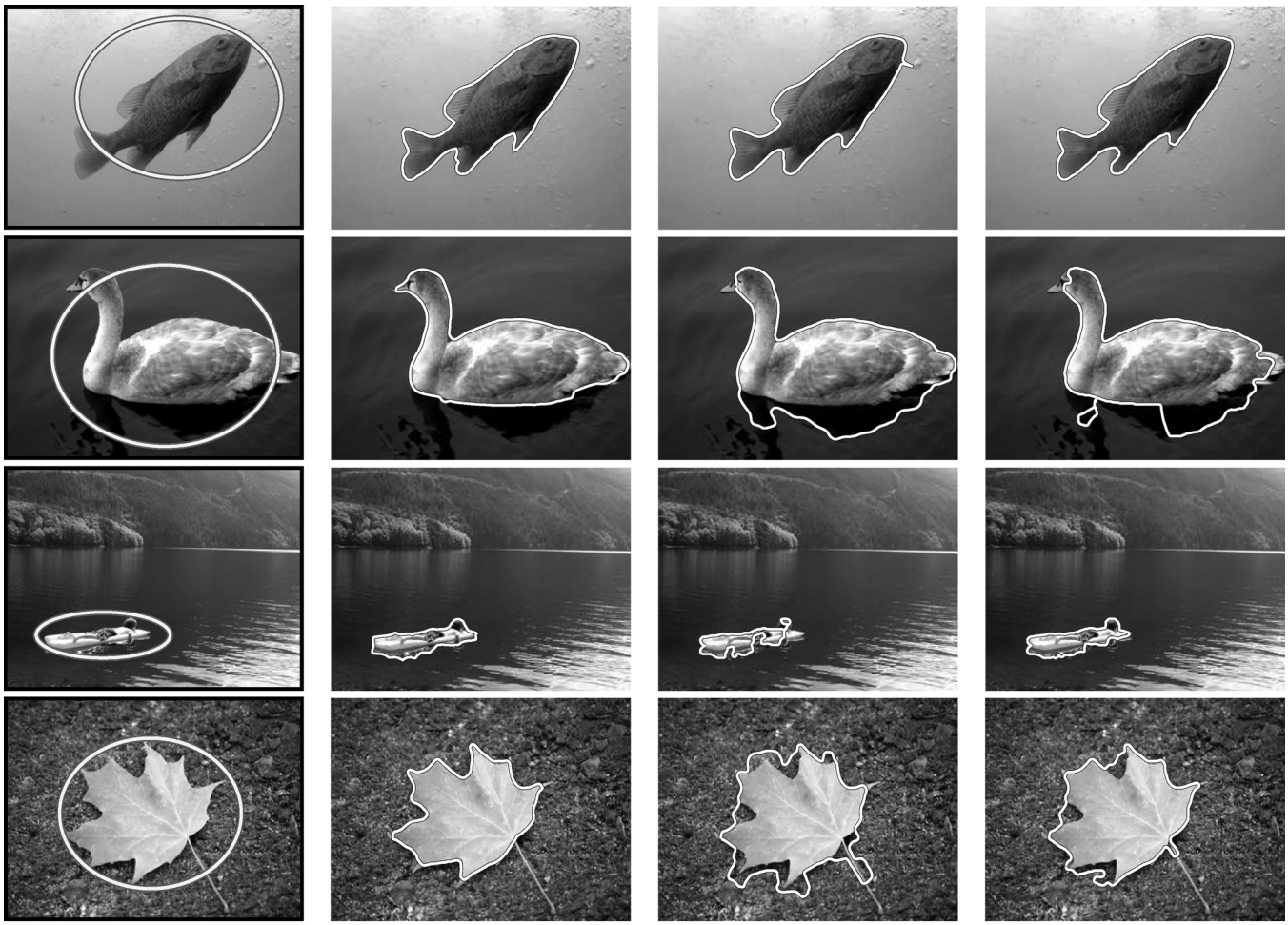

Fig. 1. Examples of detected object boundaries using KPAC, GVFS, and VFC. The first column present four images with initial solutions (FISH, DOCK, BOAT and LEAF). These four images were collected from [21]. Second, third and fourth column presents the results of KPAC, GVFS [15] and VFC [16], respectively. KPAC successfully identified the desired boundaries for all test images.

and VFC, due mainly to faster convergence speed. Examples of detected object boundaries for the tested methods are shown in Fig. 1. Visually, the boundaries determined using KPAC are better localized and more accurate than GVFS and VFC.

GVFS and VFC uses two different diffusion techniques to spread out the gradient throughout the image to attract the snake that is initialized far from the desired solution. Furthermore, both the GVFS and VFC techniques use an iterative gradient descent technique for the minimization of the snake energy. Therefore, both of these techniques still suffer the problem of being trapped in local minima. GVFS and VFC works well for images where the gradient is strong and well defined along the object boundary with little noise or clutter, such as the FISH image without added noise (Fig. 1). However, the diffusion operators of GVFS and VFC start performing poorly for cases where the gradient is ill-defined along the object boundary with respect to the rest of the image due to background clutter, noise and high curvature boundaries. In these cases, both GVFS and VFC starts becoming trapped in local minima. Therefore, GVFS and VFC failed to converge to the true object boundary for the DUCK, BOAT and LEAF images.

In case of the DUCK image, the shadows near the duck creates issues with the diffusion techniques used by GVFS and VFC, resulting in convergence towards local minima. However, in case of KPAC, the penalty on dissimilarity on intensity (14) drives the active contour towards the desired solution.

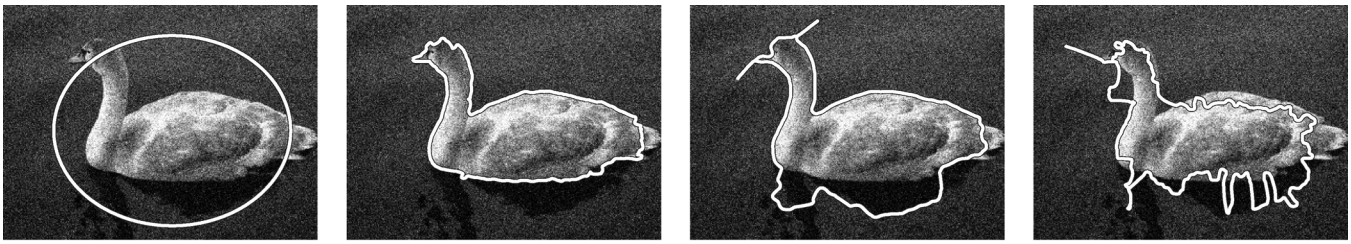

Fig. 2. Examples of detected object boundaries using KPAC, GVFS, and VFC for the DUCK image in the presence of additive Gaussian noise of standard deviation $\sigma = 40$. KPAC successfully identified the desired boundaries for noisy DUCK image, while GVFS and VFC failed to identify the boundaries correctly.

The penalty terms of KPAC are derived from image characteristics, and therefore adaptively tightens or loosens penalties to account for the high curvature boundary characteristics, noise, and background clutter. This is particularly noticeable in the LEAF image, where KPAC noticeably handles complex, high curvature boundaries and background clutter better than GVFS and VFC, both of which were trapped in local optima and thus resulted in poorly localized object boundaries. Similar difficulties handling high curvature boundaries can be seen in the fish's fin in the FISH image and the duck's bill in the DUCK image.

Finally, the visual qualitative results of KPAC compared to GVFS and VFC for the DUCK image contaminated with additive Gaussian noise of zero mean and 40 standard deviation is shown in Fig. 2. It can be observed that KPAC is able to successfully identify the desired boundaries, while GVFS and VFC both exhibit noticeable errors in the identified boundaries.

V. Conclusions

In this letter, a novel kernel-based active contour (KPAC) approach to object boundary detection was introduced. By introducing an adaptive kernel derived from underlying image characteristics into the parametric active contour approach, KPAC is able to better handle complex high curvature boundaries, noise, background clutter, as well as improve convergence speed. Future work involves extending KPAC for 3-D volume boundary detection and investigating additional local image characteristics to achieve better boundary detection performance.

References

[1] A. Mishra, A. Wong, W. Zhang, D. Clausi, and P. Fieguth, "Improved interactive medical image segmentation using enhanced intelligent scissors (eis)," in *Annu. Int. Conf. IEEE Engineering in Medicine and Biology Soc.*, Aug. 2008, pp. 3083–6.

[2] C. Davatzikos and J. Prince, "An active contour model for mapping the cortex," *IEEE Trans. Med. Imag.*, vol. 14, pp. 65–80, Mar. 1995.

[3] F. Leymarie and M. D. Levine, "Tracking deformable objects in the plane using an active contour model," *IEEE Trans. Pattern Anal. Mach. Intell.*, vol. 15, no. 6, pp. 617–634, 1993.

[4] N. Alajlan, M. Kamel, and G. Freeman, "Geometry-based image retrieval in binary image databases," *IEEE Trans. Pattern Anal. Mach. Intell.*, vol. 30, no. 6, pp. 1003–1013, 2008.

[5] S. Mahmoodi, "Shape-based active contours for fast video segmentation," *IEEE Siganl Process. Lett.*, vol. 16, no. 10, pp. 857–860, 2009.

[6] N. M. Eric and A. B. William, "Intelligent scissors for image composition," in *SIGGRAPH '95: Proc. 22nd Annu. Conf. Computer Graphics and Interactive Techniques*, New York, 1995, pp. 191–198.

[7] M. Kass, A. Witkin, and D. Terzopoulos, "Snakes: Active contour models," *Int. J. Comput. Vis.*, vol. 1, no. 4, pp. 321–331, 1988.

[8] V. Caselles, F. Catte, T. Coll, and F. Dibos, "A geometric model for active contours in image processing," *Numer. Math.*, vol. 66, pp. 1–31, 1993.

[9] R. Malladi, J. A. Sethian, and B. C. Vemuri, "Shape modeling with front propagation: A level set approach," *IEEE Trans. Pattern Anal. Mach. Intell.*, vol. 17, no. 2, pp. 158–175, 1995.

[10] P. Brigger, J. Hoeg, and M. Unser, "B-spline snakes: A flexible tool for parametric contour detection," *IEEE Trans. Image Process.*, vol. 9, pp. 1484–1496, 2000.

[11] B. Xin, Z. Chungang, and D. Han, "A new mura defect inspection way for tft-lcd using level set method," *IEEE Signal Process. Lett.*, vol. 16, no. 4, pp. 311–314, 2009.

[12] D. Schonfeld and N. Bouaynaya, "A new method for multidimensional optimization and its application in image and video processing," *IEEE Signal Process. Lett.*, vol. 13, no. 8, pp. 485–488, 2006.

[13] A. A. Amini, T. E. Weymouth, and R. C. Jain, "Using dynamic programming for solving variational problems in vision," *IEEE Trans. Pattern Anal. Mach. Intell.*, vol. 12, no. 9, pp. 855–867, 1990.

[14] A. Mishra, P. Fieguth, and D. Clausi, "Accurate boundary localization using dynamic programming on snakes," in *Can. Conf. Robotics and Computer Vision*, May 2008, pp. 261–269.

[15] C. Xu and J. Prince, "Snakes, shapes, and gradient vector flow," *IEEE Trans. Image Process.*, vol. 7, pp. 359–369, 1998.

[16] B. Li and T. Acton, "Active contour external force using vector field convolution for image segmentation," *IEEE Trans. Image Process.*, vol. 16, pp. 2096–2106, 2007.

[17] L. Cohen, "On active contour models and balloons," *Comput. Vis. Graph. Image Understand.*, vol. 53, no. 2, pp. 211–218, Mar. 1991.

[18] L. Cohen and I. Cohen, "Finite-element methods for active contour models and balloons for 2-d and 3-d images," *IEEE Trans. Pattern Anal. Mach. Intell.*, vol. 15, no. 11, pp. 1131–1147, 1993.

[19] A. Mishra, P. Fieguth, and D. Clausi, "Robust snake convergence based on dynamic programming," in *IEEE Int. Conf. Image Processing*, Oct. 2008, pp. 1092–1095.

[20] B. Saha, N. Ray, and H. Zhang, "Snake validation: A pca-based outlier detection method," *IEEE Signal Process. Lett.*, vol. 16, no. 6, pp. 549–552, 2009.

[21] S. Alpert, M. Galun, T. Basri, and A. Brandt, "Image segmentation by probabilistic bottom-up aggregation and cue integration," in *IEEE Computer . Conf. Computer Vision and Pattern Recognition*, Minneapolis, MN, USA, Jun. 2007, pp. 1–8.